J. Plasma Fusion Res. SERIES, Vol.7 (2006) 138-141

# Pulsed Laser Ablation of Hydrogen-Implanted Graphite Target

SAKAWA Youichi*, SHIBAHARA Takahiro, SATO Kouji and TANABE Tetsuo

*Graduate School of Engineering, Nagoya University, Nagoya 464-8603, Japan*

(Received: 12 October 2004 / Accepted: 28 April 2005)


### Abstract

Ablation of the $H^+$-implanted graphite target by pulsed laser irradiation with an ArF laser (193 nm, pulse length: $\tau \simeq 8$ ns, intensity: $I_L < 3 \times 10^9$ W/cm$^2$) or the fourth harmonic of a Nd:YAG laser (266 nm, $\tau \simeq 20$ ps, $I_L < 9 \times 10^{11}$ W/cm$^2$) has been investigated. The intensities for ablation threshold are $I_L \simeq 4 \times 10^8$ and $\simeq 5 \times 10^9$ W/cm$^2$ for the 193 and 266 nm lasers, respectively. Above the ablation threshold for the 266 nm laser irradiation, two ablation regions, a weakly-ablated (WA) region and a strongly-ablated (SA) region, are observed; the threshold laser intensity of $I_L \simeq 7{\times}10^{10}$ W/cm$^2$ is determined by the strong-ionization threshold of $C^+$ ions. When the target is irradiated by the 193 nm laser, only the WA region is observed; the averaged mass number of emitted ions is $\simeq 200$ for initial few shots, and the most of the implanted H atoms is released within a few 10 shots. In visible emission spectra, only $C_2$ Swan band is observed in the WA region both for the 266 and 193 nm laser irradiation. For the 266 nm laser irradiation in the SA region, the emitted ions are mostly $C^+$ and $C^{2+}$, and the optical emission of C I, C II, and C III lines are dominant. For the removal of the implanted H, the WA region seem to be suited, since a large amount of $H_2$ is released.



### Keywords:

laser ablation, graphite, tritium retention, tritium removal, ArF laser, YAG laser


## 1. Introduction

Carbon is a candidate as plasma facing materials in ITER and future D-T fusion reactors. Because of large tritium retention in carbon, a significant fraction of tritium is expected to retain in the vacuum vessel as co-deposits with carbon, and it is necessary to remove tritium periodically [1]. One of the methods to remove tritium is a laser induced desorption. Skinner *et al.* [2] have used a low-intensity ($I_L = 8 \times 10^3$ W/cm$^2$) continuous-wave Nd laser (1.06 μm) for the tritium removal from the co-deposits of the TFTR carbon tiles. Shu *et al.* have used a pulsed ArF laser (193 nm, $I_L < 3 \times 10^8$ W/cm$^2$) in the ablative conditions to remove hydrogen from the co-deposits of carbon tiles [3].

In this paper, we investigate pulsed laser ablation of the graphite target, in which 10 keV $H^+$ ion are implanted, and examine effects of laser intensity on the ablation with using an ArF excimer laser and the fourth harmonic of a Nd:YAG laser.

## 2. Experimental

Figure 1 shows the experimental setup. Experiments were conducted under the vacuum pressure $< 3 \times 10^{-8}$ Torr. A pulsed ArF excimer laser (Lambda Physik OPTex, 193 nm, energy: $E_L < 13$ mJ/pulse, pulse length: $\tau \simeq 8$ ns, $I_L < 3 \times 10^9$ W/cm$^2$, repetition rate: 5 Hz) or the fourth harmonic of a Nd:YAG laser (Continuum Custom PY61C-10, 266 nm, $E_L < 3$ mJ/pulse, $\tau \simeq 20$ ps, $I_L < 9{\times}10^{11}$ W/cm$^2$, repetition rate: 10 Hz) was focused on the target surface by a quartz lens of the focal length of 300 mm through a quartz window either with 0° or 45° direction to the normal plane of the target. We varied $I_L$ by changing both $E_L$ and the distance between the lens and the sample. A graphite plate made of IG-110U (Toyo Tanso Ltd.) was used as a target. $H^+$ ion

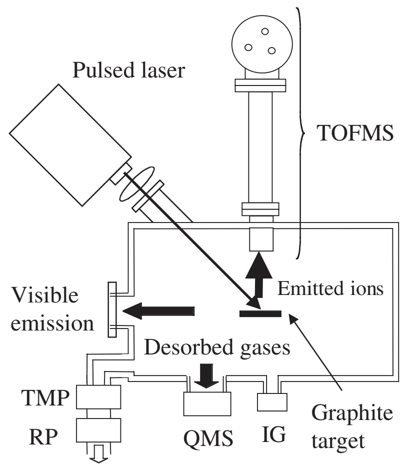


Fig. 1 Schematic view of the experimental setup.

*Corresponding author's e-mail: sakawa-y@ile.osaka-u.ac.jp*

* *Present address: Institute of Laser Engineering, Osaka University, Suita 565-0871, Japan*

beams were produced by an ion gun with the energy of 10 keV, and implanted to the target normal to the surface plane with the beam size of 8 mm in diameter. By using Transport of Ions in Matter (TRIM) code, for the implanted 10 keV $H^+$ ions with the fluence of $1 \times 10^{22}$ ions/m$^2$, it is estimated that H atoms exist 250 nm range from the surface and that the H/C ratio on the implanted area is $\simeq 0.45$. This value is similar to the H/C $\simeq 0.4$ of hydrogen co-deposited carbon film observed in carbon wall tokamaks. Emitted ions and desorbed gases were measured by a time-of-flight mass spectrometer (TOFMS) and a quadrupole mass spectrometer (QMS), respectively. Visible light emissions were also monitored by a spectrometer (Hamamatsu C7473), in which relative sensitivity on wavelength is calibrated.

## 3. Results and discussions

Integrated intensities of the $H^+$ signal of TOFMS over the first laser shot to the 50th one with the 193 nm laser irradiation for the $H^+$ implanted target are shown in Fig. 2 (a). By extrapolation, one can note a threshold for the $H^+$ emission at around $4 \times 10^8$ W/cm$^2$, which corresponds to the laser fluence of $F = 3$ J/cm$^2$. This fluence is nearly the same as the measured carbon ablation threshold of 1 J/cm$^2$ for the ArF lasers with $\tau = 25$ [3] and 15 ns [4]. Figure 2 (b) shows the intensities of the $H^+$ signal of TOFMS for the first 266 nm laser shot. The threshold intensity is around $5 \times 10^9$ W/cm$^2$. The $H^+$ signal intensity decreases by increasing $I_L$ at $I_L > 2.5 \times 10^{10}$ W/cm$^2$.

Visible emission spectrum from the $H^+$ implanted target for the 193 nm laser irradiation with $I_L = 2.3 \times 10^9$ W/cm$^2$, which is above the ablation threshold, is displayed in Fig. 3 (a). We observed only $C_2$ Swan band ($d^3\Pi_g - a^3\Pi_u$) emission, for example at 469.7, 516.5, and 589.9 nm; but optical emissions from C (C I), $C^+$

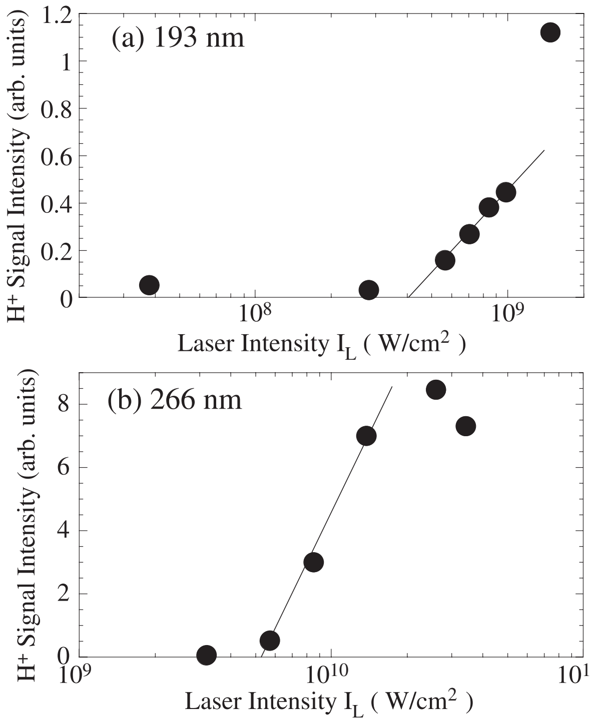


Fig. 2 (a) Integrated intensities of the $H^+$ signal of TOFMS over the first laser shot to the 50th one with the 193 nm laser irradiation, and (b) intensities of the $H^+$ signal of TOFMS for the first 266 nm laser shot, for the $H^+$ implanted target. Lines are guide to the eyes.

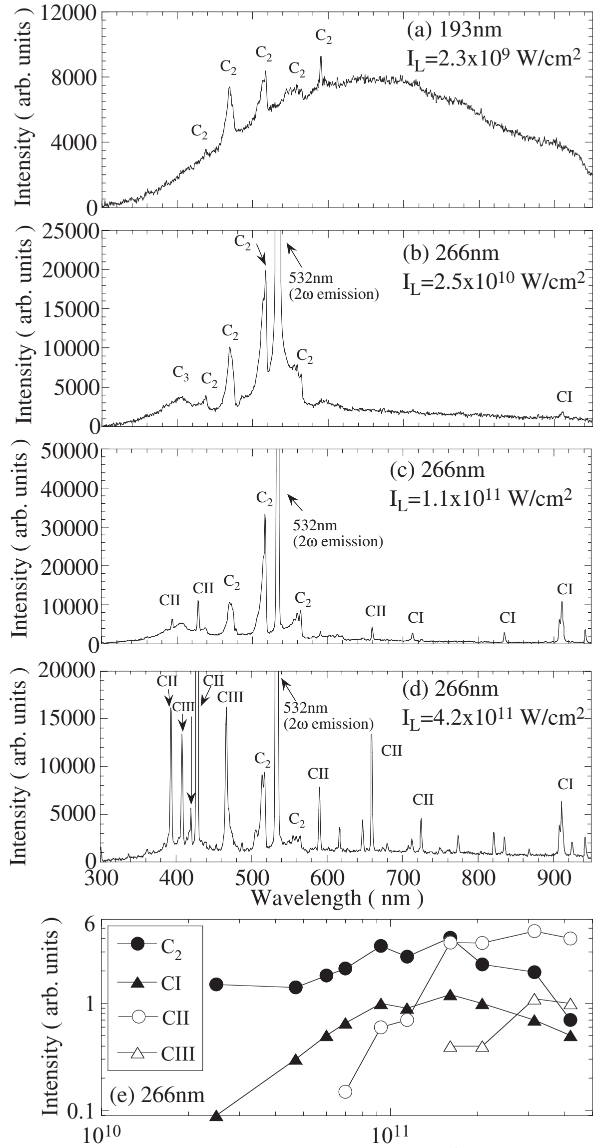


Fig. 3 Visible emission spectra from the $H^+$ implanted target for (a) the 193 nm laser irradiation with $I_L = 2.3 \times 10^9$ W/cm$^2$; and for the 266 nm laser irradiation with (b) $I_L = 2.5 \times 10^{10}$, (c) $1.1 \times 10^{11}$, and (d) $4.2 \times 10^{11}$ W/cm$^2$, respectively. (e) Intensities of the optical emission, C III (407.0 nm), C II (426.7 nm), C I (909.4 nm), and $C_2$ (516.5 nm) as a function of $I_L$.

(C II), or $C^{2+}$ (C III) were not observed. We call this ablation region as a weakly-ablated (WA) region. Figures 3 (b) − 3 (d) show visible emission spectra for the 266 nm laser irradiation with $I_L = 2.5 \times 10^{10}$, $1.1 \times 10^{11}$, and $4.2 \times 10^{11}$ W/cm$^2$, respectively, which are all above the ablation threshold. When $I_L < 2.5 \times 10^{10}$ W/cm$^2$, only $C_2$ Swan band and $C_3$ emission were observed; it is in the WA region. By increasing $I_L$, C I, C II, and C III emission appeared in this order. Intensities of the optical emission, C III(407.0 nm), C II(426.7 nm), C I(909.4 nm), and $C_2$(516.5 nm) as a function of $I_L$, are displayed in Fig. 3 (e). The threshold intensities for the appearance of C I, C II, and C III are $\simeq 2.5 \times 10^{10}$, $\simeq 7 \times 10^{10}$, and $\simeq 1.6 \times 10^{11}$ W/cm$^2$, respectively. At $I_L \simeq 7 \times 10^{10}$ W/cm$^2$, not only emission of C II started to appear but also $C^+$ signal intensity of TOFMS drastically increased, i.e., strong ionization of carbon occurred. We call the ablation region at $I_L > 7 \times 10^{10}$ W/cm$^2$ for the 266 nm laser irradiation as a strongly-ablated (SA) region.

Figures 4 (a) and 4 (b) show the mass distributions of the emitted ions when the $H^+$ implanted target was irradiated by the 193 nm laser with $I_L = 3.8 \times 10^7$ and $1.5 \times 10^9$ W/cm$^2$, respectively, at the second, 10th, and 1000th laser shots. For $I_L = 1.5 \times 10^9$ W/cm$^2$, which is in the WA region, the signal intensities of TOFMS were more than an order of magnitude larger than that for $I_L = 3.8 \times 10^7$ W/cm$^2$ (below the ablation threshold), and the averaged mass number of the released ions was smaller. This indicates that when $I_L$ is larger, the size of the emitted ion clusters is smaller due to the fragmentation in the ablated plume. When $I_L = 1.5 \times 10^9$ W/cm$^2$, the signal intensities of $H^+$ became the noise level after the initial 30 shots for the $H^+$ implanted target; while for the un-implanted target the $H^+$ intensity decreased much faster than that for the $H^+$ implanted target. $H^+$ signal intensity was remained the noise level for the un-implanted target, even when $I_L = 1.5 \times 10^9$ W/cm$^2$.

Figures 5 (a) and 5 (b) display the mass distributions of the emitted ions at the first and 900th laser shots, respectively, when the $H^+$ implanted target was irradiated by the 266 nm laser with $I_L = 5.5 \times 10^9$ W/cm$^2$. At this laser intensity, which is in the WA region, the ion mass distributions and the visible emission spectrum are somewhat similar to those for the 193 nm laser irradiation with $I_L \simeq 2 \times 10^9$ W/cm$^2$, as shown in Figs. 4 (b) and 3 (a), respectively. Figures 5 (c) and 5 (d) represent the ion mass distributions at the first and the 900th laser shots, respectively, with $I_L = 2.9 \times 10^{11}$ W/cm$^2$ (in the SA region). Only $C^+$ and $C^{2+}$ ions were emitted. Note that the absolute intensity of $C^+$ signal in the SA region [Figs. 5 (c) and 5 (d)] is more than two orders of magnitude larger than that in the WA region [Figs. 5 (a) and 5 (b)]. The visible emission spectrum at this laser intensity, is similar to that shown in Fig. 3 (d), where C II and C III emissions are dominant.

Before the laser irradiation, QMS signals were dominated by residual gases, mostly $m/e = 18$ ($H_2O$),

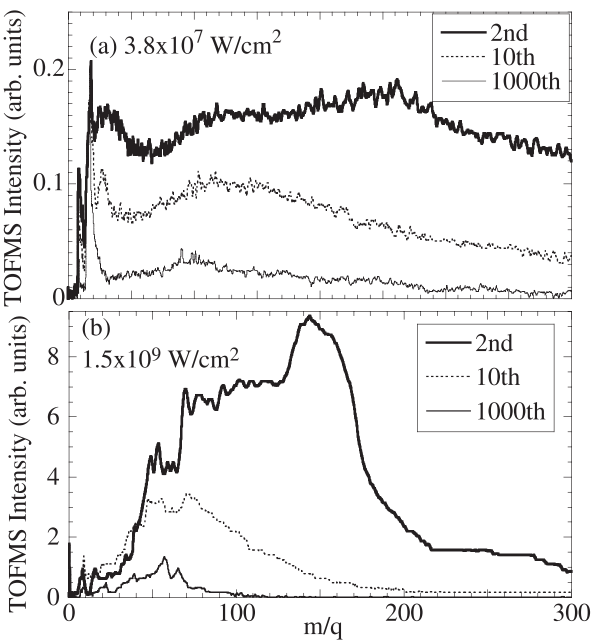


Fig. 4 Mass distributions of the emitted ions at the second, 10th, and 1000th laser shots measured by TOFMS when the $H^+$ implanted target was irradiated by the 193 nm laser with (a) $I_L = 3.8 \times 10^7$ (below the ablation threshold) and (b) $1.5 \times 10^9$ W/cm$^2$ (in the WA region).

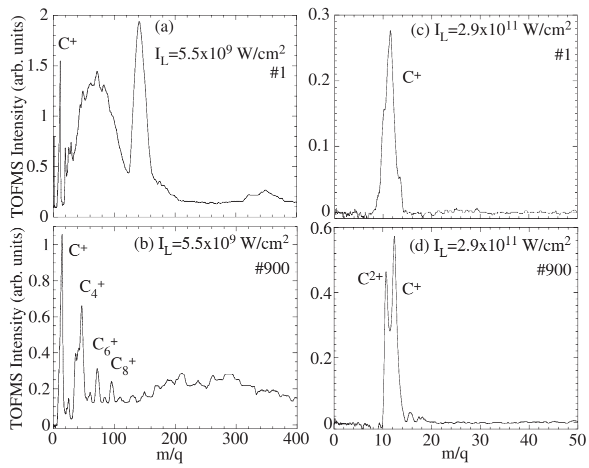


Fig. 5 Mass distributions of the emitted ions at (a) the first and (b) 900th laser shots measured by TOFMS when the $H^+$ implanted target was irradiated by the 266 nm laser with $I_L = 5.5 \times 10^9$ W/cm$^2$ (in the WA region). Mass distributions of the emitted ions at (c) the first and (d) 900th laser shots with $I_L = 2.9 \times 10^{11}$ W/cm$^2$ (in the SA region).

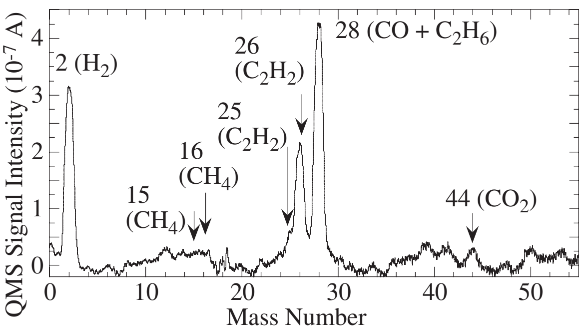


Fig. 6 Mass distribution of desorbed gases for the $H^+$ implanted target after several shots of the 266 nm laser irradiation with $I_L = 1.8 \times 10^{11}$ W/cm$^2$ (in the SA region). Signal intensities before the laser shot were subtracted from those after the laser shot.

17 (OH), 2 ($H_2$), 28 (CO), and 44 ($CO_2$). Mass distribution of desorbed gases for the $H^+$ implanted target after several shots of the 266 nm laser irradiation with $I_L = 1.8\times10^{11}$ W/cm$^2$ (in the SA region), by subtracting that before the laser shot, is shown in Fig. 6. The dominant mass numbers of the desorbed gases are $m/e = 2$ ($H_2$) and 26 ($C_2H_2$), 28 ($CO+C_2H_6$), and 44 ($CO_2$). The QMS signal intensities of $H_2$ and $C_2H_2$ increased drastically at $I_L \simeq 4 \times 10^9$ W/cm$^2$, which is close to the ablation threshold intensity derived from Fig. 2 (b). The signal intensities of both $H_2$ and $C_2H_2$ peaked at $I_L \simeq 1.3 \times 10^{10}$ W/cm$^2$, which is in the WA region, and decreased by increasing $I_L$; similar trend as the $H^+$ signal intensity shown in Fig. 2 (b). $I_L = 1 - 2 \times 10^{10}$ W/cm$^2$ in the WA region seem to be an optimum laser intensity, since a large amount of $H_2$ is released.

When the $H^+$ implanted target was irradiated by the 193 nm laser with $I_L = 1.5 \times 10^9$ W/cm$^2$, the measured mass distribution of desorbed gases was similar to that shown in Fig. 6, i.e., the ratio of the $H_2$ and $C_2H_2$ signal intensities was similar to each other in the WA and SA regions. The signal intensities of both $H_2$ and $C_2H_2$ decreased with the laser shot number and became steady state within 30 shots. In the WA region, no clear differences in the amount of $H_2$-desorption were observed between the 193 and 266 nm laser irradiation.

## 4. Conclusions

We have studied ablation of the $H^+$-implanted graphite target by irradiation of pulsed 193 and 266 nm lasers. Two ablation regions, the WA and SA regions, are distinguished for the 266 nm laser irradiation, while only the WA region is observed in the 193 nm case. For the removal of the implanted H, the WA region seem to be suited, since a large amount of $H_2$ is released.

## References

[1] G. Federici *et al.*, J. Nucl. Mater. **266-269**, 14 (1999).

[2] C.H. Skinner *et al.*, J. Nucl. Mater. **301**, 98 (2002).

[3] W.M. Shu *et al.*, J. Nucl. Mater. **313-316**, 584 (2003).

[4] A. Mechler *et al.*, Appl. Surf. Sci. **154**, 22 (2000).